Late Mississippian (early Serpukhovian) carbon isotope record of northern Laurussia: A proposal for the Viséan/ Serpukhovian boundary

Andrey V. Zhuravlev*, Yadviga A. Vevel, Denis A. Gruzdev, and Andrey V. Erofeevsky

Institute of Geology FIC Komi SC UB RAS, 54 Pervomayskaya, Syktyvkar, 167000 Russia.
** micropalaeontology@gmail.com*

ABSTRACT

The fauna provincialism in the Viséan/Serpukhovian boundary interval led to the appearance of some problems with the tracing of this boundary with biostratigraphic methods. Therefore, it is important to determine auxiliary non-biostratigraphic markers of the boundary. The article is focused on the evaluation of the correlation potential of carbon isotope excursions near the Viséan/Serpukhovian boundary, with special attention to the northern Laurussia region. The biostratigraphically constrained carbon isotope record is revealed from the terminal Viséan - lower Serpukhovian (Mississippian) shelf successions of the northern Laurussia (six key sections located in the north of Urals and Cis-Urals, NE Europe). Onset of a negative excursion in the middle part of the *Lochriea ziegleri* conodont Zone (lower Serpukhovian) shows amplitude of 1–2‰ and high spatial stability, and can be used as a stratigraphic marker in regional and global correlations.

Keywords: Carbon isotope stratigraphy; Viséan/Serpukhovian boundary; Mississippian Carboniferous; Laurussia; Urals.

RESUMEN

El provincialismo faunístico en el intervalo del límite Viseano/ Serpukhoviano provocó la aparición de algunos problemas en el trazado de este límite con métodos bioestratigráficos. Por lo tanto, es importante determinar marcadores auxiliares no bioestratigráficos de este límite. El artículo se centra en la evaluación del potencial de correlación de las excursiones de isótopos de carbono cerca del límite Viseano/Serpukhoviano, con especial atención a la región norte de Laurussia. Se reporta el registro de isotópico de carbono para secciones con control bioestatigráfico de las sucesiones de la plataforma del Viseano superior-Serpukhoviano inferior (Mississipiano) del norte de Laurussia (seis secciones de referencia ubicadas en el norte de los Urales y Cis-Urales, NE de Europa). El inicio de una excursión negativa en la parte media de la zona de conodontos de Lochriea ziegleri (Serpukhoviano inferior) muestra una amplitud de 1–2‰ y una alta estabilidad espacial, y puede usarse como marcador estratigráfico en correlaciones regionales y globales.

Palabras clave: estratigrafía de isótopos de carbono; límite Viseano/ Serpukhoviano; Mississippiano Carbonífero; Laurussia; Urales.

INTRODUCTION

The late Viséan–Serpukhovian interval corresponds to a significant biodiversity crisis in the Mississippian probably caused by onset of the Late Palaeozoic Ice Age (Fielding *et al*., 2008; Valdez Buso *et al*., 2020; Yao *et al*., 2022). During this time, the marine benthos was affected by prominent diversity reduction (Yao *et al*., 2022). In contrast, conodont diversity moderately increased in the early Serpukhovian (Zhuravlev, 2019). However, this rise of diversity was accompanied by increasing provincialism, even in the tropical realm.

This situation led to some problems with choosing a biostratigraphic marker for the Viséan/Serpukhovian boundary. As a result of active debates, a level at FAD (First Appearance Datum) of conodont species *Lochriea ziegleri* Nemirovskaya, Perret *et* Meischner in the lineage *Lochriea nodosa* (Bischoff) – *L. ziegleri* Nemirovskaya, Perret *et* Meischner had been proposed as a potential marker of the boundary (Richards and Task Group, 2005; Richards *et al*., 2011; Richards, 2013; Sevastopulo and Barham, 2014). Unfortunately, this species has a rare occurrence outside the Paleothetys realm that prevents its use for wide correlations (Qi *et al*., 2014; Herbig, 2017). Ammonoids and foraminifers in the Viséan–Serpukhovian boundary interval demonstrate provincialism as well (Bishop *et al*., 2009; Groves *et al*., 2012; Sevastopulo and Barham, 2014; Cózar *et al*., 2019). This provincialism led to the appearance of some problems with the tracing the Viséan/Serpukhovian boundary with biostratigraphic methods (*e.g.*, Herbig, 2017). Therefore, it is of current interest to determine

Zhuravlev, A.V., Vevel, Y.A., Gruzdev, D.A., Erofeevsky, A.V., 2023, Late Mississippian (early Serpukhovian) carbon isotope record of northern Laurussia: A proposal for the Viséan/ Serpukhovian boundary: Revista Mexicana de Ciencias Geológicas, v. 40, núm. 1, p. 35-43.

DOI: http://dx.doi.org/10.22201/cgeo.20072902e.2023.1.1722

auxiliary non-biostratigraphic markers of the boundary. The carbon isotope excursions seem to be promising in this respect. Liu and co-authors (2022) elucidated wide but distinguishable positive carbon isotope excursion near the boundary. It starts in the uppermost Viséan and ends in the *L. ziegleri* conodont Zone within the lower Serpukhovian. This positive excursion is bounded by two narrow negative excursions having amplitudes of about 1–2‰. These carbon isotope excursions are clearly distinguished in several South China successions and biostratigraphically well constrained (Chen *et al.*, 2016; Liu *et al.*, 2022).

This article is focused on the evaluation of the correlation potential of the carbon isotope excursions near the Viséan/Serpukhovian boundary, with special attention to the northern Laurussia region (north-eastern Europe).

GEOLOGICAL SETTING

The study area occupies the eastern margin of the Pechora platform and the western part of Urals fold-thrust belt (Figure 1). The foredeep of the Urals fold-thrust belt is filled with siliciclastic lower Ordovician, predominantly carbonate middle Ordovician–Lower Devonian, siliciclastic Middle Devonian, carbonate-siliciclastic Upper Devonian-Lower Permian, and siliciclastic Middle Permian–Triassic deposits, which were folded and faulted during the late Variscan orogeny (Puchkov, 2010). The foredeep is separated from the fold-thrust belt by a thrust fault (Puchkov, 2010) and is complicated by several fold-thrust structures (Yudin, 1994).

In the late Mississippian time, an intrashelf depression of tectonic origin occupied the eastern part of the foredeep and the western part of the Urals. The depression was separated from the Uralian Strait by a belt of isolated carbonate platforms (Gruzdev, 2017), and bounded by a shallow-water carbonate ramp to the west. Carbonate and, locally, sulfate deposits sedimented in the depression due to arid climate in the region during the late Mississippian (Boucot *et al.*, 2013).

This study is based on investigations of Viséan/Serpukhovian boundary beds in six sections located in the northern Cis-Urals and Polar Urals. The locations of the sections are reported in Appendix Table A1. These sections correspond to a wide spectrum of facies, from the shallow-water nearshore (inner ramp) to deep-water intra-shelf depression and offshore isolated carbonate platform. Shallow-water inner ramp facies crop out in the Kamenka sections (southern part of the Pechora-Kozhva swell) (Vevel *et al.*, 2017; Zhuravlev *et al.*, 2022). The outer ramp facies were studied in the Izyayu section (Tchernyshev Swell) (Kossovaya *et al.*, 2001). The facies of intra-shelf depression were studied in the Mississippka section (Sub-Polar Urals) (Sobolev *et al.*, 2015). The deposits of the isolated carbonate platform crop out in the Bolshaya Nadota section (Polar Urals) (Skompski *et al.*, 2001; Gruzdev, 2017).

Shallow-water inner ramp (the Kamenka section)

The Kamenka section include Viséan/Serpukhovian boundary beds (outcrop #99), part of the lower Serpukhovian *L. ziegleri* Zone (outcrop #125), and the upper Serpukhovian *G. bollandensis* Zone (outcrop #130). The boundary beds comprise an alternation of light-grey wavy-bedded limestones and light-grey laminated limy clay (Figure 2). The limestones yielded the foraminifers *Earlandia minor* (Rauser), *Paraarchaediscus convexus* Grozdilova *et* Lebedeva, *P. pauxillus* (Schlykova), *P.* aff. *grandiculus* (Schlykova), *Archaediscus krestovnikovi* Rauser, *Asteroarchaediscus rugosus* (Rauser), *Biseriella parva* (N. Tchernysheva), *Endostaffella parva* (Moeller), *Mediocris mediocris* (Vissarionova), *M. breviscula* (Ganelina), *Pseudotaxis* sp., *Eostaffella* sp., *Eostaffella* ex gr. *prisca* Rauser, *E. mosquensis* Vissarionova, *Diplosphaerina minima* (Suleimanov), *Pachysphaerina pachisphaerica* (T. Pronina), *Calligella antropovi* (Lipina), calcareous algae as *Koninckopora inflata* (Koninck), and rare conodonts *Taphrognathus varians* Branson *et* Mehl, *Mestognathus* cf. *bipluti* Higgins, *Cavusgnathus naviculus* (Hinde), *Lochriea senckenbergica* Nemirovskaya, Perret *et* Meischner, *Lochriea ziegleri* Nemirovskaya, Perret *et* Meischner, *Gnathodus bilineatus* (Roundy), and *Ligonodina* sp. (Zhuravlev *et al.*, 2022). The FODs of *Lochriea senckenbergica* Nemirovskaya, Perret, Meischner (Figure 3) and *Lochriea ziegleri* Nemirovskaya, Perret *et* Meischner approximately mark the Viséan-Serpukhovian boundary and base of the *L. ziegleri* conodont Zone (Zhuravlev *et al.*, 2022). The upper part of the *L. ziegleri* Zone crops out in outcrop #125 located about 6 km NE of outcrop #99. This part of the Serpukhovian succession is composed of an alternation of light-grey wackestone and grainstone (Figure 2) containing abundant foraminifers *Archaesphaera* spp., *Eotuberitina reitlingerae* A.M.-Macklay, *Earlandia elegans* (Rauser *et* Reitlinger), *Pseudoammodiscus priscus* (Rauser), *Endothyra* sp., *Endostaffella* sp., *Mediocris breviscula* (Ganelina), *Pseudotaxis eominima* (Rauser), *Eostaffella postmosquensis* Kireeva, *Globivalvulina* sp., *Pseudoendothyra* cf. *kerka pressa* Durkina,

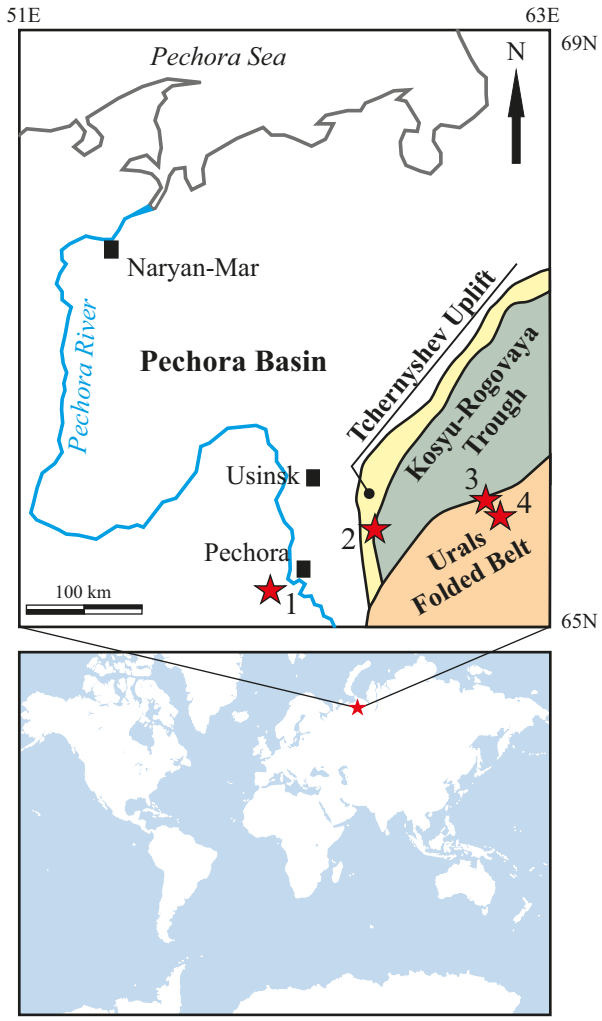

Figure 1. Locality maps. 1: Kamenka sections, Pechora Basin, shallow-water inner ramp facies; 2: Izyayu section, Tchernyshev Uplift, outer ramp facies; 3: Mississippka section, Urals Folded Belt, intrashelf depression facies; 4: Bolshaya Nadota section, Urals Folded Belt, isolated carbonate platform facies.

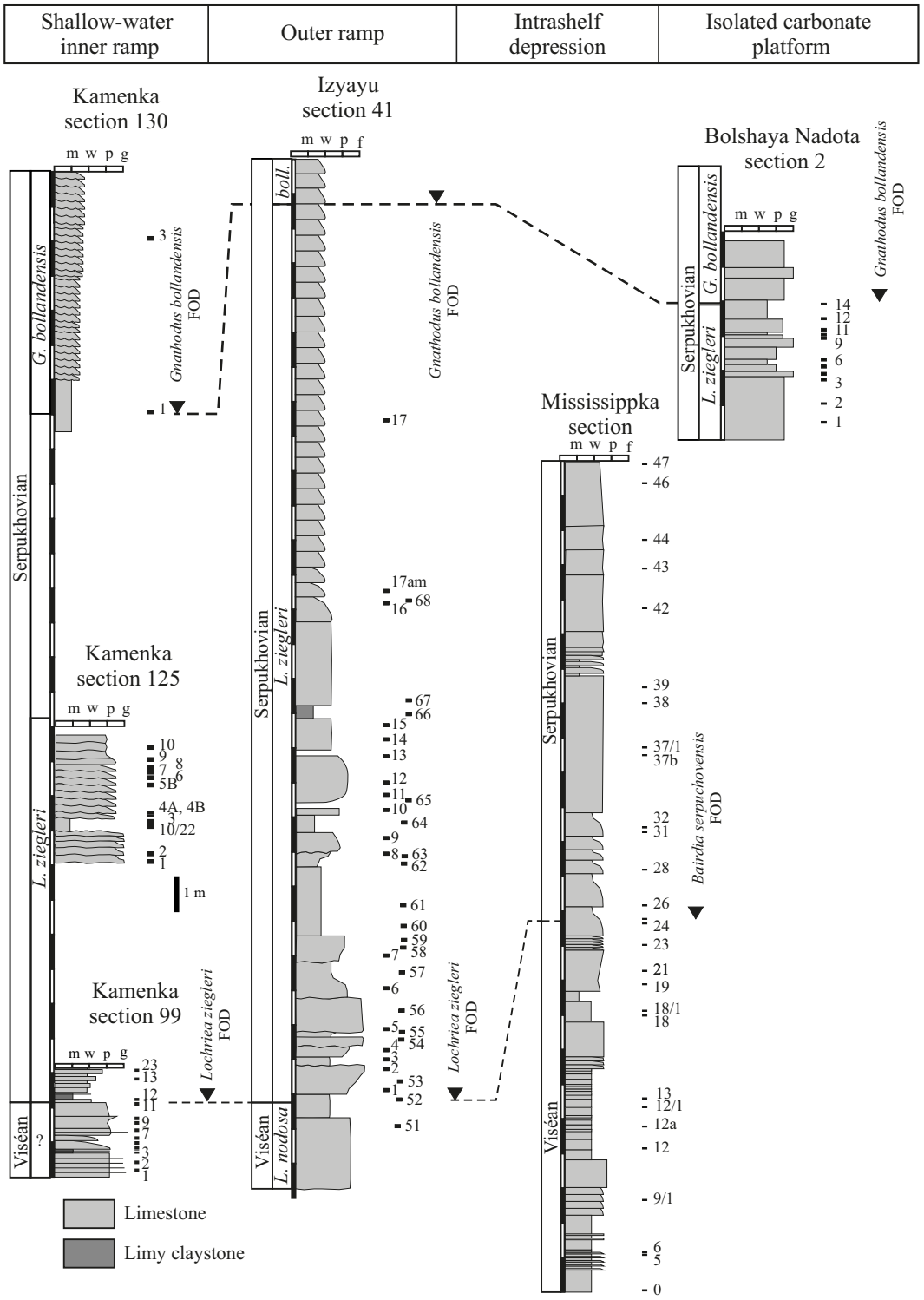

Figure 2. Correlation of the key sections of the Viséan-Serpukhovian boundary interval in the North Urals and Cis-Urals. Abbreviations: m – mudstone; w – wackestones; p – packstone; g – grainstone; f – floatstone; FOD – first occurrence datum.

Planospirodiscus sp., *Paraarchaediscus* aff. *pauxillus* (Schlykova), *Asteroarchaediscus rugosus* (Rauser), *Neoarchaediscus* sp., calcareous algae *Koninckopora*, and conodonts *Lochriea senckenbergica* Nemirovskaya, Perret *et* Meischner, *Lochriea ziegleri* Nemirovskaya, Perret *et* Meischner, *Lochriea mononodosa* (Rhodes, Austin *et* Druce), *Lochriea multinodosa* (Wirth), *Gnathodus romulus* Meischner *et* Nemirovska, *Gnathodus bilineatus* (Roundy), *Pseudognathodus homopunctatus* (Ziegler), *Mestognathus beckmanni* Bischoff, *Mestognathus bipluti* Higgins, *Cavusgnathus unicornis* Youngquist *et* Miller, *Cavusgnathus convexus* Rexroad, *Hindeodus scitulus* (Hinde), *Hindeodus cristulus* (Youngquist *et* Miller), *Idioprioniodus conjunctus* (Gunnell), *Vogelgnathus* sp., and *Kladognathus* sp. (Vevel *et al.*, 2017).

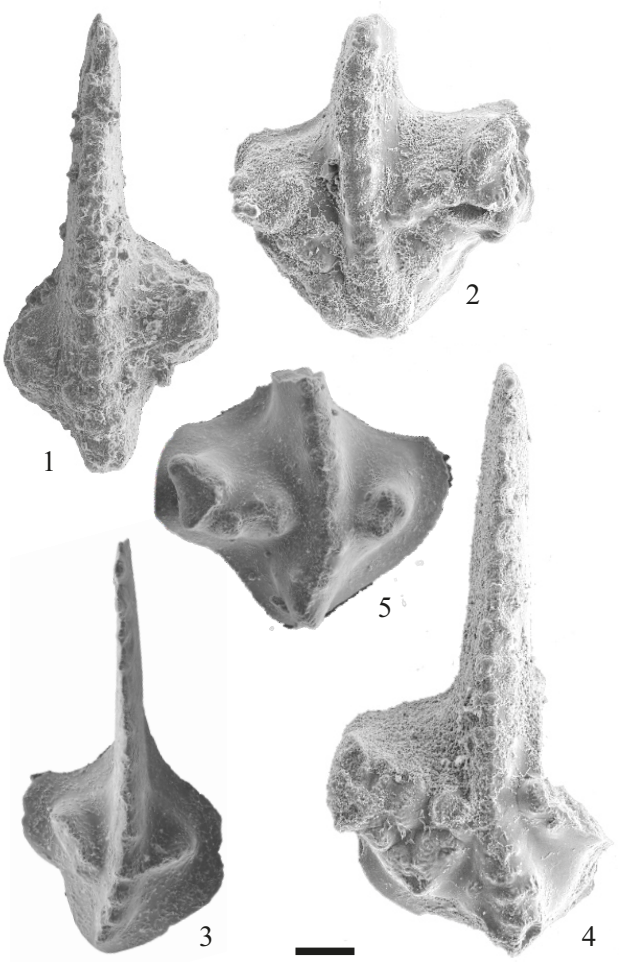

Figure 3. Lower Serpukhovian conodonts from the North Urals and Cis-Urals sections. 1: *Lochriea senckenbergica*, Kamenka river section 99, sample 99-12/19, specimen 715/20, *L. ziegleri* Zone. 2: *Lochriea ziegleri*, Kamenka river section 125, sample 125-1/16, specimen 512/11-11, *L. ziegleri* Zone. 3: *Lochriea costata* - *L. senckenbergica* transition, Izyayu River section 4, sample Iz41-17am/20, specimen 445/22, *L. ziegleri* Zone. 4: *Lochriea multinodosa*, Kamenka river section 125, sample 125-1/16, specimen 512/11-10, *L. ziegleri* Zone. 5: *Lochriea senckenbergica*, Izyayu river section 4, sample Iz4-52/98, specimen 445/11, *L. ziegleri* Zone. Scale bar is 100 μm.

The upper part of the Serpukhovian succession in outcrop #130 is composed of alternating mudstone and wacke-mudstone (Figure 2). These deposits yielded conodonts *Hindeodus scitulus* (Hinde), *Hindeodus cristulus* (Youngquist *et* Miller), *Hindeodus minutus* (Ellison), *Gnathodus remus* Meischner *et* Nemirovska, *Gnathodus bollandensis* (Higgins *et* Bouckaert), *Kladognathus complectens* (Clarke), *Cavusgnathus cristatus* Branson *et* Mehl, and *Idioprioniodus* sp., characteristic of *G.bollandensis* conodont Zone.

Outer ramp (the Izyayu section)

The outer ramp facies of the lower Serpukhovian were studied in the Izyayu section (Tchernyshev uplift). The level of the Viséan/Serpukhovian boundary had been detected in this section by FODs of the conodonts *Lochriea cruciformis* (Clarke) and *Lochriea ziegleri* Nemirovskaya, Perret *et* Meischner (Kossovaya *et al*., 2001; Zhuravlev, 2003). The Viséan part of the succession is composed of algal limestones, but the lower Serpukhovian part demonstrates a gradual transition from algal and polybioclastic limestones (mainly packstone and grainstone) to an unit composed of vague calciturbidites (wacke- and mudstones and limy clay). The calciturbidite unit comprises the upper part of the *L. ziegleri Zone* and the lower part of the *G. bollandensis* Zone (Zhuravlev, 2003) (Figure 2).

Intrashelf depression (the Mississippka section)

The Viséan/Serpukhovian boundary interval in the intrashelf depression facies crops out in a small quarry near the Mississippka river (Polar Urals). The succession is composed of vague calciturbidites (Figure 2) yielding rare conodont, foraminifer, and ostracod associations (Sobolev *et al*., 2015). The base of the Serpukhovian is approximately determined on the basis of the occurrence of the Serpukhovian ostracods *Bairdia serpuchovensis* Samoilova *et* Smirnova and *Kellettina bituberculata* (M'Coy) (Sobolev *et al*., 2015).

Isolated carbonate platform (the Bolshaya Nadota section)

The Serpukhovian sequence of the Bolshaya Nadota section is composed of an alternation of dark-gray wavy-bedded packstone and grainstone with oolites, crinoids, and calcareous algae (Figure 2). The lower part of the sequence contains Serpukhovian conodonts of the *L. ziegleri Zone*: *Gnathodus bilineatus* (Roundy), *Lochriea commutata* (Branson *et* Mehl), *Lochriea senckenbergica* Nemirovskaya, Perret *et* Meischner, *Lochriea mononodosa* (Rhodes, Austin *et* Druce), *Lochriea ziegleri* Nemirovskaya, Perret *et* Meischner, *Lochriea monocostata* (Pazukhin *et* Nemirovskaya), and *Idioprioniodus* sp.

The upper part of the sequence yields brachiopods (*Fluctuaria*), solitary rugose corals, and a conodont association of the *G. bollandensis*

Zone composed of *Lochriea commutata* (Branson *et* Mehl), *Lochriea mononodosa* (Rhodes, Austin *et* Druce), *Lochriea monocostata* (Pazukhin *et* Nemirovskaya), *Lochriea cruciformis* (Clarke), *Lochriea ziegleri* Nemirovskaya, Perret *et* Meischner, *Gnathodus bollandensis* (Higgins *et* Bouckaert), *Gnathodus girtyi soniae* Rhodes, Austin *et* Druce, and *Hindeodus scitulus* (Hinde).

MATERIAL

The sections listed above and in Appendix Table A1 were sampled for carbon and oxygen isotope analyses. A total of 84 rock samples were analyzed for the stable isotopes. The Kamenka sections were characterized by 29 samples; 16 samples were collected from the Izyayu section; 28 samples came from the Mississippka section; and 11 samples were collected from the Bolshaya Nadota section. The carbon and oxygen isotope values are reported in Appendix Table A2.

Some characteristic conodonts from the study sections are presented in Figure 3. The conodont collections #445, 512, and 715 are deposited in the Geological Museum (Syktyvkar, Russia).

METHODS

The samples for isotope analysis were collected from unaltered limestones with a stratigraphical spacing of 1–5 decimeters to several meters (Figure 2). The carbonate powder for isotope analysis was extracted from fresh surfaces of rock samples with a steel microdrill. The carbon and oxygen isotope composition of the carbonates was determined with a DELTA V Advantage mass spectrometer with sample preparation on a Gas Bench II line by standard methods. $\delta^{13}C_{carb}$ values are reported relative to the PDB (Pee Dee Belemnite) standard and $\delta^{18}O_{carb}$ values were reported relative to the SMOW (Standard Mean Ocean Water) standard. The precision of the $\delta^{13}C_{carb}$ values is ±0.04‰ and precision of the $\delta^{18}O_{carb}$ values is ±0.06‰. Isotope analysis was performed at the CKP "Geonauka" of the N.P. Yushkin Institute of Geology FC Komi SC UrB RAS (Syktyvkar, Russia). Statistical data analyses were performed using the PAST software (Hammer *et al*., 2001).

The conodont data compose the biostratigraphic framework for the studied sections. The level of the Viséan/Serpukhovian boundary is marked by the first occurrence of *Lochriea ziegleri* (Figures 2, 3). Ostracods and foraminifers provided additional biostratigraphic information in some sections with scarce content of conodont associations (*e.g.*, Mississippka section).

RESULTS

A composite screening diagram was used to evaluate the reliability of the isotope records (Zhuravlev *et al*., 2020 (Figure 4). Samples located in the doubtful area of the diagram were excluded from the following analysis; they are marked by gray circles in the isotope plots in Figure 4.

Shallow-water inner ramp (the Kamenka sections)

The carbonate carbon isotope record of the Kamenka sections reveals mean $\delta^{13}C$ values of -1.1‰. The $\delta^{13}C$ values range from -3‰ up to 0.9‰. The lowest values correspond to two intervals (Figure 4). The first interval is located just below the level of FOD (First Occurrence Datum) of the Serpukhovian conodonts *Lochriea ziegleri* (outcrop #99). In this interval, $\delta^{13}C$ values drop down to -3‰. The second interval corresponds to the *L. ziegleri* Zone (outcrop #125) and is characterized by a $\delta^{13}C$ decrease down to -2‰. These intervals are separated by $\delta^{13}C$ values of about 0‰ to +0.9‰. The uppermost part of the Serpukhovian succession (*G. bollandensis* Zone, outcrop #130) has $\delta^{13}C$ values around 0‰ (Figure 4).

Outer ramp (the Izyayu section)

The carbonate carbon isotope record of the Izyayu section comprises the lower Serpukhovian interval (Figure 4). The lowermost Serpukhovian is characterized by $\delta^{13}C$ values ranging from 2.7‰ to 3.5‰. In the upper part of the section, $\delta^{13}C$ values show a decreasing trend from about 4‰ just above the FOD of *Lochriea ziegleri* to about 2‰ in the upper part of the *L. ziegleri* Zone (Figure 4). The mean $\delta^{13}C$ value in this section is of 2.7‰. Unclear negative excursions are detected in the lowermost part of the *L. ziegleri* Zone (down to 2.7‰) and in the middle part of this zone (down to 2‰).

Intrashelf depression (the Mississippka section)

In the Mississippka section $\delta^{13}C$ values are highly variable in the Upper Viséan, but they are near monotonic in the lower Serpukhovian (Figure 4). $\delta^{13}C$ values fluctuate around 2.5‰ in the studied interval. The prominent negative excursions (down to *ca.* 1‰) occur in the Upper Viséan and lowermost Serpukhovian parts of the section. The lower Serpukhovian carbon isotope record shows a "plateau" with $\delta^{13}C$ values of about 2.5–3‰.

Isolated carbonate platform (the Bolshaya Nadota section)

In the Bolshaya Nadota section, the carbon isotope record spans a stratigraphic interval corresponding to part of the Serpukhovian *L. ziegleri* Zone. $\delta^{13}C$ values vary from 1.8‰ to 2.8‰ with minimum at the middle part of the sampled succession (Figure 4). The amplitude of the $\delta^{13}C$ negative shift in the *L. ziegleri* Zone is about 1‰.

Generally, two $\delta^{13}C$ negative excursions can be recognized in the investigated Viséan/Serpukhovian successions (Figure 4). The first excursion (SN1) occurs near the Viséan/Serpukhovian boundary and has amplitude of about 1–1.5‰. The second excursion (SN2) corresponds to the middle part of the Serpukhovian *L. ziegleri* Zone. Its amplitude varies from 0.5 up to 2.5‰.

DISCUSSION

The lack of co-variation between the $\delta^{13}C$ and $\delta^{18}O$ values of the studied carbonates (R^2=0.053, n=84) indicates that the majority of $\delta^{13}C$ values record ancient seawater compositions and can be used for isotope stratigraphy (Figure 4).

The carbon isotope pattern near the Viséan/Serpukhovian boundary in the study sections shows two moderate negative shifts (SN1 and SN2) separated by a broad positive excursion (Figure 4). The first negative excursion (SN1) is recognized below the FOD of *Lochriea ziegleri* in the Kamenka section (#99) and just above the FOD of *Lochriea ziegleri* in the Izyayu section (Figure 4). High variability of carbon isotope signal in the Viséan/Serpukhovian boundary interval of the Mississippka section prevents reliable recognition of this excursion. Probably this excursion corresponds to the negative shift of $\delta^{13}C$ just above the first occurrence of the Serpukhovian ostracodes (Figure 4). SN1 negative excursion can be recognized in the carbon isotope record of the east-central Idaho (Batt *et al*., 2007), where it occurs in the Chesterian just above Viséan/Serpukhovian boundary (Figure 4). Taking into account that SN1 excursion nearly coincides with a regression maximum (Figure 5), it seems reasonable that this excursion was partly caused by weathering intensification or local epigenetic processes, especially in the shallow-water nearshore localities (*e.g.*, the Kamenka section).

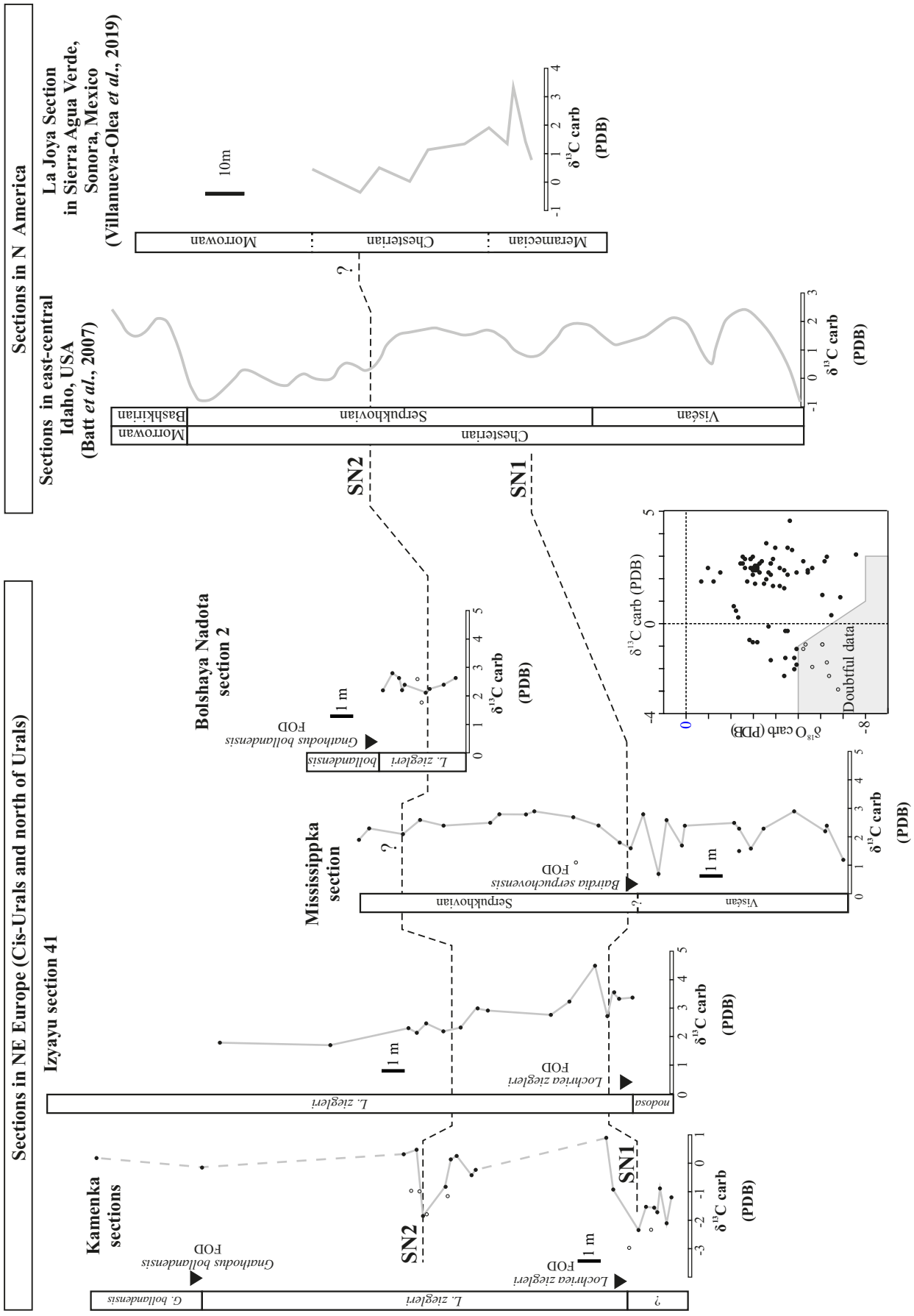

Figure 4. UpperViséan - Lower Serpukhovian carbon isotope stratigraphy of carbonate successions along the Laurussia shelves.

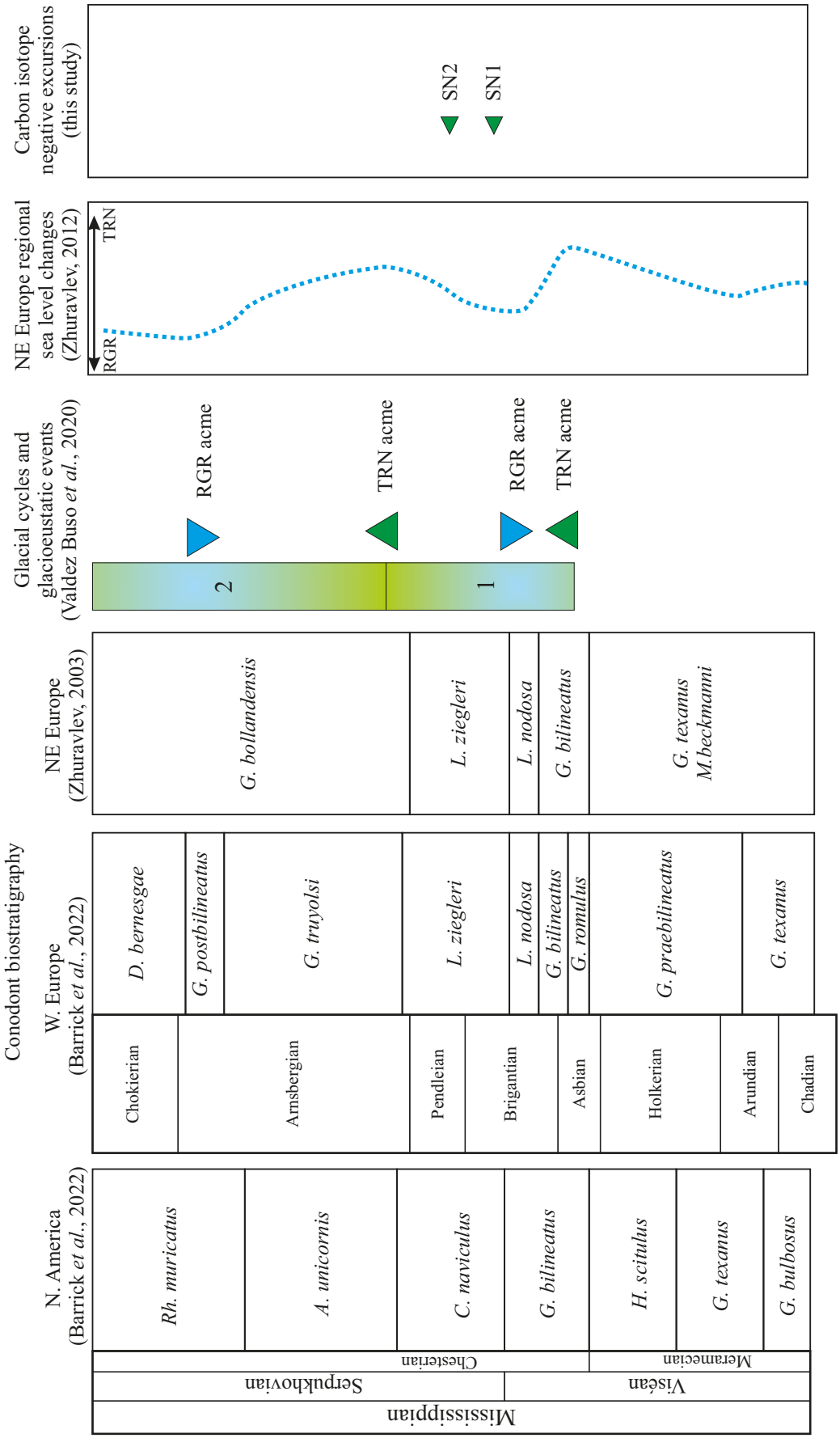

Figure 5. Conodont biostratigraphy of the upper Viséan – Serpukhovian interval, glacial cycles, regional sea level changes, and carbon isotope negative shifts (marked as SN1 and SN2).

The SN2 negative shift shows carbon isotope values of about +2‰ in offshore environment in eastern Laurussia (modern north-eastern Europe), but of about 0‰ in western Laurussia (North America (Figure 4). In spite of variations in amplitude, the SN2 isotope anomaly demonstrates high stability over the Laurussia shelves: north-eastern Europe, east-central Idaho (USA), and Sonora (Mexico) sections (Figure 4). Also, this anomaly can be distinguished in the South China successions (Paleotethys realm). It has been noted in the Shuidong section in the lower part of the *Janischewskina delicata* foraminiferal Zone, and in the Naqing section in the middle part of the *L. ziegleri* conodont Zone (Liu *et al*., 2022, fig. 10). Thus, biostratigraphically this anomaly is constrained to the middle part of the *L. ziegleri* conodont Zone (Figure 5) and the lower part of the *Janischewskina delicata* foraminiferal Zone.

The high volatility of $\delta^{13}C$ values in the Viséan/Serpukhovian boundary interval makes it difficult to distinguish individual excursions. Therefore, reliable correlation of the SN1 excursion over the world is problematic. In contrast, the $\delta^{13}C$ record in the lower Serpukhovian (*L. ziegleri* Zone) is smoother, and SN2 excursion can be recognized more reliably. Similarities in the variations of carbon isotope record in the northeastern (north Urals basin) and western (Idaho and Sonora) shelves of Laurussia suggest that the causes of these variations were global in nature.

According to Yao *et al*. (2022), the series of the carbon isotope excursions near the Viséan/Serpukhovian boundary coincides with the onset of the major Late Palaeozoic Ice Age. It comprises the upper part of the *L. nodosa* Zone and the lower part of the *L. ziegleri* Zone (Figure 5). Also, SN1 and SN2 excursions correspond to the middle part of the Glacial cycle 1 of Valdez Buso *et al*. (2020), and to the terminal Viséan – early Serpukhovian glacioeustatic regression (Figure 5).

Numerous explanations of the nature of negative excursions of inorganic carbon isotopic composition have been proposed (see Pisarzowska and Racki, 2020 for a review). Processes that could lead to low $\delta^{12}C$ values include: increase in organic-carbon weathering, collapse of the biological pump, extensive wildfires, episodes of hydrothermal activity in the basin, and freshwater plumes caused by melting of ice caps (Pisarzowska and Racki, 2020). In the case of the lower Serpukhovian negative excursions SN1 and SN2, increase in organic-carbon weathering provoked by regression and extensive freshwater plumes initiated by melting of ice caps during short term deglaciation pulses seem to be the most realistic causes. In any case, high spatial stability of these excursions suggests that their causes were sub-global or global in nature. Therefore, these excursions constrained by *L. ziegleri* conodont Zone can be used as reliable stratigraphic markers in the Laurussia realm.

CONCLUSIONS

The carbon isotope variations near the Viséan/Serpukhovian boundary promise a useful tool for intercontinental correlation. The onset of the negative excursion in the middle part of the *L.ziegleri Zone* (SN2) (approximately corresponds to the lower part of *Janischewskina delicata* foraminiferal Zone) shows an amplitude of 1–2‰, high spatial stability along the Laurussia shelves, and can be used as a stratigraphic marker.

APPENDIX

Tables A1 and A2 can be downloaded from the web site of this journal <www.rmcg.unam.mx> in the abstract's page of this paper.

ACKNOWLEDGEMENTS

Authors thank Irina V. Smoleva for helpful assistance in isotope studies, and reviewers for providing constructive comments and recommendations toward the improvement of the manuscript.

REFERENCES

Barrick, J.E., Alekseev, A.S., Blanco-Ferrera, S., Goreva, N.V., Hu, K., Lambert, L.L., Nemyrovska, T.I., Qi, Y., Ritter, S.M., Sanz-López, J., 2022, Carboniferous conodont biostratigraphy: London, Geological Society, Special Publications, 512(1), 695-768, DOI: 10.1144/SP512-2020-38 .

Batt, L.S., Montañez, I.P., Isaacson, P., Pope, M.C., Butts, S.H., Abplanalp, J., 2007, Multi-carbonate component reconstruction of mid-carboniferous (Chesterian) seawater $\delta^{13}C$: Palaeogeography, Palaeoclimatology, Palaeoecology, 256, 298-318, https://doi.org/10.1016/j.palaeo.2007.02.049

Bishop, J.W., Montañez, I.P., Gulbranson, E.L., Brenckle, P.L., 2009, The onset of mid-Carboniferous glacio-eustasy: sedimentologic and diagenetic constraints, Arrow Canyon, Nevada: Palaeogeography, Palaeoclimatology, Palaeoecology, 276, 217-243.

Boucot, A.J., Chen, Xu, Scotese, C.R., 2013, Phanerozoic Paleoclimate: An Atlas of Lithologic Indicators of Climate: SEPM Concepts in Sedimentology and Paleontology (Print-on-Demand Version), 11, 478 pp.

Chen, J., Montañez, I.P., Qi, Y., Wang, X., Wang, Q., Lin, W., 2016, Coupled sedimentary and $\delta^{13}C$ records of late Mississippian platform-to-slope successions from South China: Insight into $\delta^{13}C$ chemostratigraphy: Palaeogeography, Palaeoclimatology, Palaeoecology, 448, 162-178.

Cózar, P., Vachard, D., Aretz, M., Somerville, I.D., 2019, Foraminifers of the Viséan – Serpukhovian boundary interval in Western Palaeotethys: a review: Lethaia, 52, 260-284, DOI: 10.1111/let.12311

Fielding, C.R., Frank, T.D., Isbell, J.L., 2008, The late Paleozoic ice age — a review of current understanding and synthesis of global climate patterns, *in* Fielding, C.R., Frank, T.D., Isbell, J.L. (eds.), Resolving the Late Paleozoic Ice Age in Time and Space: Geological Society of America Special Paper 441, 343-354, DOI: 10.1130/2008.2441(24)

Groves, J.R., Yue, W., Yuping, Q., Richards, B.C., Ueno, K., Xiangdong,W., 2012, Foraminiferal biostratigraphy of the Viséan–Serpukhovian (Mississippian) Boundary Interval at slope and platform sections in Southern Guizhou (South China): Journal of Paleontology, 86, 753-774.

Gruzdev, D.A., 2017, The Late Devonian-Early Carboniferous isolated carbonate platform in the Subpolar Urals (Bol'shaya Nadota River): Vestnik IG Komi SC UB RAS, 4, 16-23, DOI: 10.19110/2221-1381-2017-4-16-23 (in Russian)

Hammer, Ø., Harper, D.A.T., Ryan, P.D., 2001, PAST: Paleontological statistics software package for education and data analysis: Palaeontologia Electronica, 4(1), 9 pp., http://palaeo-electronica.org/2001_1/past/issue1_01.htm

Herbig, H.-G., 2017, Taxonomic and stratigraphic problems concerning the conodonts *Lochriea senckenbergica* Nemirovskaya, Perret & Meischner, 1994 and *Lochriea ziegleri* Nemirovskaya, Perret & Meischner, 1994 – consequences for defining the Viséan-Serpukhovian boundary: Newsletter on Carboniferous Stratigraphy, 33, 28-35.

Kossovaya, O.L., Vevel, Y.A., Zhuravlev, A.V., 2001, Fauna and sedimentation near the Viséan/Serpukhovian boundary in the Izyayu Section, Tchernyshev Swell, Polar Urals: Newsletter on Carboniferous Stratigraphy, 19, 29-31.

Liu, C., Vachard, D., Du, Y., Munnecke, A., Liang, T., 2022, Foraminiferal Zonation and Carbon Isotope Stratigraphy Through the Viséan–Serpukhovian Boundary Interval — New Data from Three Inner-Platform Successions of South China: Available at SSRN: https://ssrn.com/abstract=4063138 or http://dx.doi.org/10.2139/ssrn.4063138

Pisarzowska, A. and Racki, G., 2020, Chapter 8 - Comparative carbon isotope chemostratigraphy of major Late Devonian biotic crises, in Montenari, M. (ed.), Carbon Isotope Stratigraphy: Stratigraphy and timescale, 5, 387-466, DOI: 10.1016/bs.sats.2020.08.001

Puchkov, V.N., 2010, Geology of the Urals and Cis-Urals (actual problems

of stratigraphy, tectonics, geodynamics and metallogeny): Ufa, DesignPoligraphService, 280 pp. (in Russian), available at http://ig.ufaras.ru/File/PubTxt/books/Puchkov2010.pdf

Qi, Y., Nemyrovska, T., Wang, X., Chen, J., Wang, Z., Lane, H., Wang, Q., 2014, Late Visean – early Serpukhovian conodont succession at the Naqing (Nashui) section in Guizhou, South China: Geological Magazine, 151(2), 254-268, DOI:10.1017/S001675681300071X

Richards, B.C., 2013, Current status of the International Carboniferous Time Scale: New Mexico Museum of Natural History and Science, Bulletin, 60, 348-353.

Richards, B.C., Task Group, 2005, The Viséan–Serpukhovian boundary: a summary of progress made on research goals established at the XV ICCP Carboniferous Workshop in Utrecht: Newsletter on Carboniferous Stratigraphy, 23, 7-8.

Richards, B.C., Aretz, M., Barnett, A., Barskov, I., Blanco-Ferrera, S., Brenckle, P.L., Clayton, G., Dean, M., Ellwood, B., Gibshman, N., Hecker, M., Konovalova, V.A., Korn, D., Kulagina, E., Lane, R., Mamet, B., Nemyrovska, T., Nikolaeva, S.V., Pazukhin, V., Qi, Y.-P., Sanz-López, J., Saltzman, M.R., Titus, A., Utting, J., Wang, X., 2011, Report of the Task Group to establish a GSSP close to the existing Viséan-Serpukhovian boundary: Newsletter on Carboniferous Stratigraphy, 29, 26-30.

Sevastopulo, G.D., Barham, M., 2014, Correlation of the base of the Serpukhovian Stage (Mississippian) in NW Europe: Geological Magazine, 152, 244-253.

Skompski, S., Paszkowski, M., Krobicki, M., Kokovin, K., Korn, D., Tomas, A., Wrzolek, T., 2001, Depositional setting of the Devonian/Carboniferous biohermal Bol'shaya Nadota Carbonate Complex, Subpolar Urals: Acta Geologica Polonica, 51(3), 217-235.

Sobolev, D.B., Zhuravlev, A.V., Popov, V.V., Vevel, Y.A., 2015, The depression type of the Upper Visean–Serpukhovian succession in the Subpolar Urals: Lithosphere (Russia), 4, 62-72. (in Russian, with English abstract).

Valdez Buso, V., Milana, J.P., di Pasquo, M., Paim, P.S.G., Philipp, R.P., Aquino, C.D., Cagliari, J., Chemale, F., Junior, Kneller, B., 2020, Timing of the Late Palaeozoic glaciation in western Gondwana: New ages and correlations from Paganzo and Paraná basins: Palaeogeography, Palaeoclimatology, Palaeoecology, 544, 109624. DOI: 10.1016/j.palaeo.2020.109624

Vevel, Y.A., Gruzdev, D.A., Zhuravlev, A.V., 2017, Foraminifers and conodonts of shallow-water deposits of the early Serpukhovian age in the Kamenka River section (south of Pechora-Kozhva megaswell): Syktyvkar palaeontological miscellany, 9, 14-23.

Villanueva-Olea, R., Barragán, R., Palafox-Reyes, J.J., Jiménez-López, J.C., Buitrón-Sánchez, B.E., 2019, Microfacies and stable isotope analyses from the Carboniferous of the La Joya section in Sierra Agua Verde, Sonora, Mexico: Boletín de la Sociedad Geológica Mexicana, 71(3), 585-607, DOI: 10.18268/BSGM2019v71n3a1

Yao, L., Jiang, G., Mii, H.-S., Lin, Y., Aretz, M., Chen, J., Qi, Y., Lin, W., Wang, Q., Wang, X., 2022, Global cooling initiated the Middle-Late Mississippian biodiversity crisis: Global and Planetary Change, 215, 103852, DOI: 10.1016/j.gloplacha.2022.103852

Yudin, V.V., 1994, Orogenesis of the North Urals and Pay-Khoy: Ekaterinburg, Russia, Nauka, 284 pp. (in Russian)

Zhuravlev, A.V., 2003, Konodonty verhnego devona–nizhnego karbona Severo-Vostoka Evropejskoj Rossii: Saint-Petersburg, Russia, VSEGEI, 85 pp. (in Russian)

Zhuravlev, A.V., 2012, Sedimentation model of the transitional zone from the Elets to Lemva Formation Belts (Devonian-Carboniferous boundary, Cis-Polar Ural): Neftegasovaa geologia. Teoria i practica, 7(4), http://www.ngtp.ru/rub/2/59_2012.pdf (in Russian, with English abstract)

Zhuravlev, A.V., 2019, Dynamics of the conodont diversity in the Late Devonian–Early Carboniferous (Famennian–Serpukhovian): Lithosphere (Russia), 19(1), 81–91, DOI: 10.24930/1681-9004-2019-19-1-81-91 (in Russian, with English abstract).

Zhuravlev, A.V., Plotitsyn, A.N., Gruzdev, D.A., Smoleva, I.V., 2020, Carbon isotope stratigraphy of the Tournaisian (Lower Mississippian) successions of NE Europe, *in* Montenari, M. (Ed.), Carbon Isotope Stratigraphy. Stratigraphy & Timescales 5 Chapter 9: Cambridge, Academic Press, 467–528.

Zhuravlev, A.V., Gerasimova, A.I., Vevel, Y.A., Erofeevsky, A.V., Gruzdev, D.A., 2022, Preliminary data on the Viséan-Serpukhovian boundary beds in the Kamenka River section (Pechora Swell, NE Europe): Newsletter on Carboniferous Stratigraphy, 36, 22-24.

Manuscript received: november 9, 2022
Corrected manuscript received: january 11, 2023
Manuscript accepted: january 12, 2023